

A hybrid variational quantum circuit approach for stabilizer states classifiers

Hamma Aslam[†], Frédéric Holweck^{†,‡}

[†] Laboratoire Interdisciplinaire Carnot de Bourgogne, UMR 6303 CNRS,

University of Technology of Belfort-Montbéliard, 90010 Belfort Cedex, France and

[‡] Mathematics and Statistics Department, Auburn University, Auburn, AL, USA

(Dated: November 13, 2025)

Entanglement classification of pure multipartite quantum states is a challenging problem in quantum information theory that can be mathematically stated as orbit classification for some given group action on the ambient Hilbert space. The group action depends on the grained classification one expects, the finer-grained one being the classification up to local unitary transformation (LU). In this article, we show how a variational quantum circuit approach can be used to learn entanglement orbits, and we apply our findings to build a classifier for four-qubit states.

I. INTRODUCTION

Quantum entanglement has gained much attention in recent years due to its role as a fundamental resource in many quantum information applications including quantum cryptography [1], quantum teleportation [2], and quantum error correction [3]. Quantum computation protocols that demonstrate a quantum speed-up in problem solving also rely heavily on entanglement [4, 5]. The characterization and classification of entangled quantum states is thus of significant importance and has been widely studied [6–9]. One of the most common methods of entanglement classification is based on equivalence relations of local operations, which often include Local Unitary (LU), Local Operations and Classical Communications (LOCC), and Stochastic Local Operations and Classical Communications (SLOCC) [10, 11]. When restricting to graph states, the group of Local Clifford operations (LC), a subgroup of LU, is relevant. Under this framework, all states that are related by the action of a group (e.g. LU, LOCC, SLOCC, LC) are said to belong to the same orbit or the same equivalence class. Being a non-local property, the action of local operations leaves the intrinsic nature of entanglement unchanged and states belonging to the same orbit have similar entanglement properties.

Classifying an unknown quantum state based on its orbit often requires a complete knowledge of the state. Even classical machine learning methods, that have been successfully employed for this purpose [12, 13], require some information of the quantum state that can be used as input to the model, which can be very challenging due to the closed nature of quantum systems. One way to obtain this information is through quantum state tomography [14]. This method can be very noisy and resource intensive since it requires measurements whose numbers scale exponentially with the number of subsystems. Another method called quantum state discrimination, which uses Positive Operator-Valued Measurements (POVM),

can also be used to gain information about a state [15]. Unfortunately, finding the optimal POVMs can be a very complicated and resource intensive task.

In light of these difficulties, a variational quantum circuit approach to entanglement classification appears to be a natural solution. When using a Variational Quantum Classifier (VQC), the quantum circuit operations can be applied directly on the quantum system to be classified, thereby eliminating the need for information extraction through resource intensive measurements. The natural Hilbert space in which these quantum circuits operate also allows a polynomial scaling of the resources with the number of subsystems. Furthermore, since VQCs outsource the computationally intensive optimization to a classical computer, they can be readily executed on Noisy Intermediate-Scale Quantum (NISQ) era hardware.

Extensive prior work has been done on variational quantum classification of entangled states [16–19]. However, most of it uses classification methods based on entanglement witnesses or measures. While there have been attempts at classifying entanglement based on local operation orbits [20], they have been restricted in a manner that does not explore the full equivalence class and reduces the problem to a linear classification problem.

The rest of the paper is arranged as follows with Section II giving some basic background on VQCs and entanglement classification of pure states. Section III discusses the non-linearity of orbits and the manner in which a hybrid VQC approach can learn these non-linear orbits much better than a simple VQC. Section IV demonstrates our approach by applying this hybrid VQC to learn various classification schemes of four-qubit graph states including the LC and LU orbit identification. Finally, Section V discusses directions for future work.

II. BACKGROUND

We review in this section some basic notions on variational quantum circuits and entanglement classification of pure states

A. VQC

The classification of entangled states using a Variational Quantum Classifier (VQC) can be categorized as a supervised quantum machine learning task [16, 21]. The first essential component of such tasks is a labeled dataset of the form $\{\mathbf{x}_i, y_i\}$ with \mathbf{x}_i being the feature vector of the input quantum state $|\psi_i\rangle$, and y_i being the corresponding label. Here, the feature vector \mathbf{x}_i is the d -dimensional amplitude vector of the quantum state $|\psi_i\rangle \in \mathcal{S} \subseteq \mathcal{H}$, such that $|\psi_i\rangle$ is an n -qubit pure quantum state with $d = 2^n$. Since we only focus on binary classification, the labels considered are $y_i \in \{-1, 1\}$. The VQC acts as a parametrized function $f(\mathbf{x}_i; \boldsymbol{\theta})$ which is trained to predict the labels by varying $\boldsymbol{\theta}$, with the goal often being the generalization of this function to unseen datasets.

A schematic representation of a general VQC is shown in FIG. 1, where the first block of operations $G(\mathbf{x}_i)$ represents the encoding of the feature vector \mathbf{x}_i into the quantum circuit. Following that, repeated layers of some combination of parametrized rotation gates and entangling gates, represented by $U(\boldsymbol{\theta})$ are implemented. Finally, a measurement over some observable A is conducted to extract the model's predicted label $y'_i(\mathbf{x}_i; \boldsymbol{\theta})$ from the quantum circuit

$$\langle A \rangle = \langle \psi_o | G^\dagger(\mathbf{x}_i) U^\dagger(\boldsymbol{\theta}) A U(\boldsymbol{\theta}) G(\mathbf{x}_i) | \psi_o \rangle = y'_i(\mathbf{x}_i; \boldsymbol{\theta}) \quad (1)$$

where $|\psi_o\rangle = |00..0\rangle$ is the initial state of the circuit. To quantify the success of the model's prediction, a cost function is defined as

$$C(\mathbf{x}_i; \boldsymbol{\theta}) = \frac{1}{m} \sum_{i=1}^m (y_i - y'_i(\mathbf{x}_i; \boldsymbol{\theta}))^2 \quad (2)$$

with m being the total number of samples in the dataset. This makes the task of classification into an iterative optimization task such that

$$\boldsymbol{\theta}_{opt} = \arg \min_{\boldsymbol{\theta}} C(\mathbf{x}_i; \boldsymbol{\theta}) \quad (3)$$

Within the VQC, both the cost function calculation and optimization are executed on a classical computer.

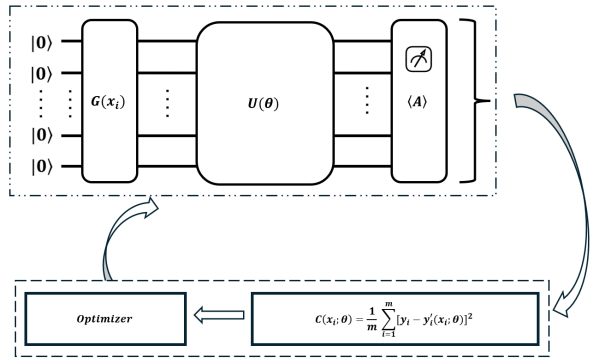


FIG. 1: Schematic diagram of a general n -qubit simple Variational Quantum Classifier. The pattern \cdots indicates execution on a quantum device and $\dashv\dashv$ indicates execution on a classical device.

B. Entanglement classification

One knows since the early 2000s that for $n \geq 3$, pure quantum states can exhibit entanglement in non-equivalent ways [10]. *Non-equivalent* means that two states cannot be transformed into each other by local operations. Conversely, *equivalent* states are those that can be interconverted by local operations, and are therefore regarded as belonging to the same entanglement class. All states $|\psi'\rangle$ equivalent to a given state $|\psi\rangle$ under a group action G are said to belong to the G -orbit of $|\psi\rangle$. The type of local operations considered depends on the desired granularity of the classification. Let us first introduce two standard schemes of classifications:

- 1. Local Unitary (LU):** $LU = SU_2(\mathbb{C})^{\times n}$. Here the group LU acts on \mathcal{H}_n as the product of local unitaries. We say $|\psi\rangle \equiv_{LU} |\psi'\rangle$ if and only if there exist $A_i \in SU_2(\mathbb{C})$, $i = 1, \dots, n$, such that

$$|\psi\rangle = A_1 \otimes \dots \otimes A_n |\psi'\rangle.$$

The LU classification is a fine grained one. Note that for pure states, LU equivalence coincides with LOCC (Local Operations with Classical Communication [10]) equivalence.

- 2. Stochastic Local Operations and Classical Communication (SLOCC):** $SLOCC = SL_2(\mathbb{C})^{\times n}$. Here the restriction to unitaries is relaxed: local operators are only required to be invertible. Thus, $|\psi\rangle \equiv_{SLOCC} |\psi'\rangle \Leftrightarrow \exists A_i \in SL_2(\mathbb{C})$, $i = 1, \dots, n$, such that

$$|\psi\rangle = A_1 \otimes \dots \otimes A_n |\psi'\rangle.$$

Example 1 Up to LU equivalence, any two-qubit pure

state $|\psi\rangle \in \mathcal{H}_2$ can be brought to its Schmidt form

$$|\psi\rangle \equiv_{LU} \sqrt{\lambda_0}|00\rangle + \sqrt{\lambda_1}|11\rangle,$$

with $\lambda_0, \lambda_1 \in \mathbb{R}_+$ and $\lambda_0 + \lambda_1 = 1$. This yields a continuum of LU classes parametrized by $\lambda_1 \in [0, 1/2]$: the case $\lambda_1 = 0$ corresponds to the class of separable states, while $\lambda_1 = 1/2$ corresponds to the maximally entangled class represented by the well-known EPR state,

$$|EPR\rangle = \frac{1}{\sqrt{2}}(|00\rangle + |11\rangle)[22].$$

In contrast, up to SLOCC equivalence, there are only two orbits: the orbit of separable states (all states SLOCC-equivalent to $|00\rangle$) and the orbit of entangled states (all states equivalent to $|EPR\rangle$).

Example 2 For $n = 3$, LU equivalence allows one to reduce a three-qubit state to the form

$$|\psi\rangle = \lambda_0|000\rangle + \lambda_1 e^{i\phi}|100\rangle + \lambda_2|101\rangle + \lambda_3|110\rangle + \lambda_4|111\rangle,$$

with $\lambda_i \geq 0$, $\phi \in [0, 2\pi]$, and $\sum \lambda_i^2 = 1$, leading again to infinitely many LU orbits [9].

For the SLOCC classification [10], the three-qubit Hilbert space decomposes into six classes:

- the orbit of separable states (SLOCC. $|000\rangle$),
- three biseparable orbits (SLOCC. $|0\rangle \otimes |EPR\rangle$, SLOCC. $\frac{1}{\sqrt{2}}(|000\rangle + |101\rangle)$, SLOCC. $|EPR\rangle \otimes |0\rangle$),
- the W class (SLOCC. $\frac{1}{\sqrt{3}}(|100\rangle + |010\rangle + |001\rangle)$),
- and the GHZ class (SLOCC. $\frac{1}{\sqrt{2}}(|000\rangle + |111\rangle)$).

For $n \geq 4$, both LU and SLOCC classifications contain infinitely many orbits [11]. The SLOCC classification of pure states remains tractable for $n = 4$ [23, 24], but becomes intractable in full generality for $n \geq 5$ [25].

III. LEARNING ORBITS

A. Non-linearity

The orbit closure of a state $|\psi\rangle$ under a group action G is an algebraic variety defined by the vanishing of some set of polynomial equations. For LU and SLOCC, such polynomials are typically non-linear and the corresponding orbits under their action reflect this non-linearity [12, 26].

Learning these non-linear orbits is especially difficult for simple VQCs since all the quantum gates applied within the quantum circuit are linear unitary transformations. This difficulty is demonstrated in FIG. 2 with the use of a simple synthetic linearly non-separable two-dimensional dataset.

B. A hybrid VQC

There are many ways to deal with this non-linearity issue in VQCs, the most notable of which include non-linear feature maps [21] and exploitation of the tensor product structure of the quantum circuit [27]. Unfortunately, non-linear feature maps often require full knowledge of the input feature vector, which is very resource-intensive as mentioned before, and exploitation of tensor product structure requires significantly scaling up the number of qubits. A method that does not have either of these drawbacks is the use of classical neural network (NN) layers for post-processing.

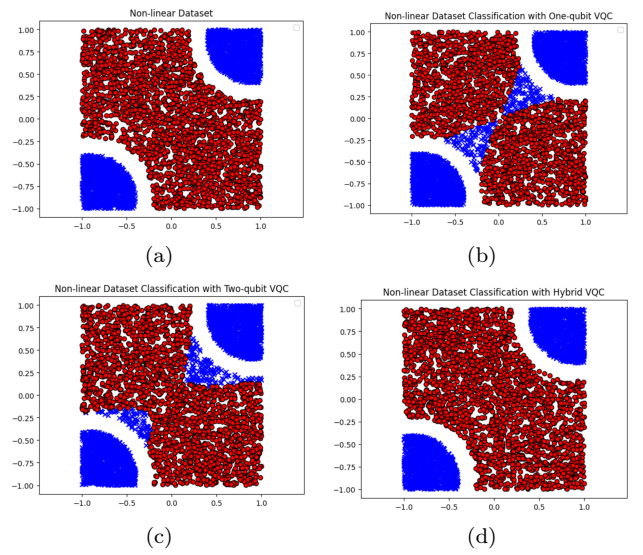


FIG. 2: (a) shows the original classification of the dataset. (b) shows the results when a single-qubit VQC is trained to classify this dataset. It can be observed that this VQC can only draw linear boundaries in its attempt to minimize the cost function. (c) shows the results when a two-qubit VQC is trained to classify the dataset. The two features of the dataset were encoded into the amplitudes [28] of the qubits with the other two amplitudes treated as free hyperparameters and set to 0 and 0.25. However, it is obvious that even with these additional degrees freedom, this VQC cannot fully grasp the non-linearity required from the problem. Finally, (d) shows the performance of a two-qubit hybrid VQC that conducts classical post-processing using classical NN layers. The classification accuracy is 100% for this case.

To conduct this post-processing, a separate measurement can be performed on each of total n qubits and the resulting n -dimensional output vector $\mathbf{y}'_i(\mathbf{x}_i; \theta)$ can then be passed on to classical NN layers as input. The number of layers and the number of neurons in each of these layers can be varied. If there are h neurons in the first layer and $W \in \mathbb{R}^{h \times n}$, $\mathbf{b} \in \mathbb{R}^h$ are trainable parameters, then the action of the first layer involves the implementation

of a non-linear activation function σ as

$$\mathbf{y}'_i(\boldsymbol{\theta}) \xrightarrow{\text{layer}} \sigma(W\mathbf{y}'_i(\boldsymbol{\theta}) + \mathbf{b}) \quad (4)$$

Here, σ acts element-wise on the entries such that $\sigma(\mathbf{z}) = [\sigma(z_1), \sigma(z_2), \dots]$. The non-linearity provided by this activation function can significantly improve the action of the variational classifier on linearly non-separable datasets as can be seen in FIG. 2.

Once this post-processing is done, the output of the final classical NN layer: $y_i^C(\mathbf{x}_i; W, \mathbf{b}, \boldsymbol{\theta})$, can be provided to the cost function and the optimizer can update the trainable parameters in the quantum circuit as well as the classical NN layers. A schematic diagram of the specific hybrid VQC structure employed in this work, along with its classical post-processing layers is shown in FIG. 3 for the general case of n -qubits.

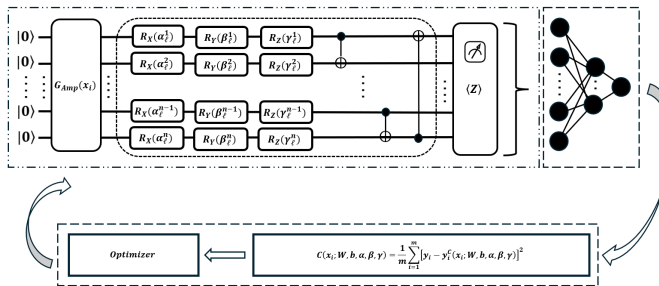


FIG. 3: Schematic n -qubit diagram of the specific hybrid VQC structure employed in this work. Here, $\boldsymbol{\theta} = \{\alpha, \beta, \gamma\}$ form the set of trainable parameters of the quantum circuit with their upper and lower indices indicating the qubit number and layer number respectively. G_{AMP} indicates amplitude encoding [28] and R_X, R_Y, R_Z are single qubit rotation gates round X, Y, Z axes respectively. The diagram only shows one hidden layer of the classical NN for simplicity. In practice, the number of hidden layers and the number of neurons in the hidden layers were varied for each classification task. The pattern \cdots indicates execution on a quantum device, $\overline{\cdots}$ indicates repeated layer of the quantum circuit, and $\overline{\overline{\cdots}}$ indicates execution on a classical device.

In practice, the hybrid VQC was implemented in PennyLane using their `TorchLayer` class that allows the variational circuit to be treated as a Torch layer, which can then be used in combination with classical NN layers to create hybrid models within Torch's `Sequential` or `Module` classes. Since the outputs of the variational circuit were expectation values ranging from -1 to 1 , the `tanh` activation function was used in the classical layers. The optimizer used was Adam and the learning rate was varied between 0.01 to 0.001 for each learning task.

This type of post-processing not only improves the ability of the VQC to classify linearly non-separable

State Name	Training Accuracy	Test Accuracy
Fully Separable	99%	98%
Biseparable (AB-C)	98%	97%
Biseparable (A-BC)	98%	97%
Biseparable (B-AC)	99%	99%
W	100%	100%

TABLE I: Training and test accuracy results for the classification of LU orbit of three-qubit GHZ state ($\frac{1}{\sqrt{2}}(|000\rangle + |111\rangle)$) against the LU orbits of some other well known three-qubit states.

datasets, it also increases the number of trainable parameters significantly without increasing the width or depth of the quantum circuit. Thus, this architecture is especially well-suited for the complex task of classifying the local operations' non-linear orbits.

This suitability can be demonstrated with a very simple example where states are classified by the hybrid VQC into either the LU orbit of the three-qubit GHZ state or the LU orbit of one of the other three-qubit states mentioned in TABLE I. The same table shows the results of this classification, revealing that the hybrid VQC can indeed identify the states and thus learn the non-linear orbits with very high accuracy. However, since the classifier was trained to recognize only two LU orbits, instead of identifying one LU orbit from the full state space, this problem is relatively simple. A more thorough and complicated approach can thus be taken by training the hybrid VQC to learn and classify an LU orbit from the entire Hilbert space. The results for this type of classification are shown in TABLE II, which show that the classifier also does a good job of identifying the non-linear orbits even when presented with random states from the full state space.

State Name	Training Accuracy	Test Accuracy
Fully Separable	90%	89%
Biseparable (AB-C)	98%	97%
Biseparable (A-BC)	100%	99%
Biseparable (B-AC)	97%	95%
W	84%	83%
GHZ	97%	97%

TABLE II: Training and test accuracy results for the classification of LU orbits of various three qubit states against the full 3 qubit Hilbert space.

IV. APPLICATIONS

To illustrate our approach better, we apply it to the study of orbits of four-qubit graph states under different classification schemes of varying complexity. First,

we consider the set of all four-qubit graph states and show how our hybrid VQC can be trained to distinguish their entanglement classes (IV A). Next, instead of the orbits of graph states themselves, we examine the orbits of graph states under Local Clifford (*LC*) operations. For four-qubits [35], the orbit $LC \cdot |\psi_G\rangle$ of a given graph state $|\psi_G\rangle$ corresponds to the set of all stabilizer states *LU*-equivalent to $|\psi_G\rangle$ (IV B). Finally, we consider the full *LU*-orbits of the six representatives of the four-qubit graph state classification and demonstrate that our trained circuit successfully distinguishes them for each other but also from any generic states (IV C).

A. The four-qubit graph states classification

Graph states are multipartite quantum states described by a graph. Consider a graph $G = (V, E)$ with $|V|$ vertices labeled by integers $i \in \{0, \dots, |V| - 1\}$ and $|E|$ edges. The graph state $|\psi_G\rangle$ associated with G is a $|V|$ -qubit quantum state defined by

$$|\psi_G\rangle = \prod_{e \in E} CZ_e \cdot |+\rangle^{\otimes |V|},$$

where CZ_e is a controlled- Z gate acting on qubits i and j when e is the edge connecting vertices i and j .

Graph states play an important role in quantum information theory. They have applications in quantum error correction [29], quantum secret sharing [30], and measurement-based quantum computation.

Up to local transformations, a classification of graph states is known for up to $n = 12$ qubits [31]. For four qubits, there are $2^6 = 64$ different graph states, which fall into six distinct equivalence classes under local transformations (FIG. 4).

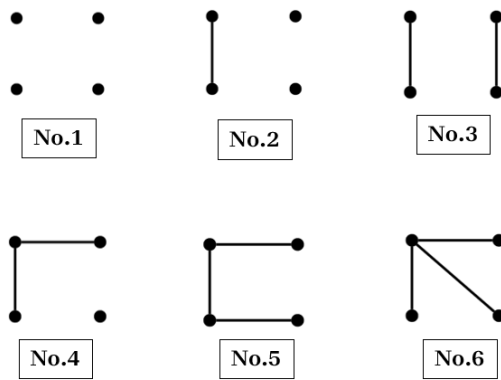


FIG. 4: Classification of four-qubit graph states. Note that the star graph corresponds to the four-qubit GHZ state.

The canonical form of those graph states is $|\psi_G\rangle = \sum_{x_1, x_2, x_3, x_4 \in \{0, 1\}} (-1)^{f_G(x_1, x_2, x_3, x_4)} |x_1 x_2 x_3 x_4\rangle$

where the function f_G is a boolean function with monomial $x_i x_j$ appearing for each CZ_{ij} . In the following table we provide examples of four-qubit states *LU* equivalent to each representative of the class as well as the number of graphs equivalent to it (up to permutation and local operations).

class N°	$f_G(x_1, x_2, x_3, x_4)$	# of <i>G</i> -states in the class	LU-equivalent four-qubit state
1	0	1	$ 0000\rangle$
2	$x_1 x_2$	6	$ EPR\rangle \otimes 00\rangle$
3	$x_1 x_2 + x_3 x_4$	3	$ EPR\rangle \otimes EPR\rangle$
4	$x_1(x_2 + x_3)$	16	$ GHZ\rangle \otimes 0\rangle$
5	$x_1 x_2 + x_2 x_3 + x_3 x_4 + x_3 x_4$	33	$\frac{1}{2}(0000\rangle + 0111\rangle + 1011\rangle + 1100\rangle)$
6	$x_1 x_2 + x_1 x_3 + x_1 x_4$	5	$ GHZ_4\rangle$

TABLE III: Class, example of representative (normal form) and number of equivalent graph states

We trained our hybrid VQC to identify these six different classes of four-qubit graph states. For the dataset, the amplitude vectors of all possible graph states were first generated. Then 50% of the samples, labeled -1, were picked from the class to be identified and the other 50%, all labeled 1, were picked uniformly from the rest of the classes. Note that, due to the limited number of graph states, repetitions were allowed while picking the samples.

The dataset was split evenly into training and test samples, with the results of the classification shown in TABLE IV. It can be observed that our hybrid VQC does an excellent job of identifying each class with an accuracy close to 100% in almost all cases.

class N°	Training Accuracy	Test Accuracy
1	100%	100%
2	100%	100%
3	99%	99%
4	98%	98%
5	98%	98%
6	100%	100%

TABLE IV: Training and test accuracy results for identification of entanglement classes of four-qubit graph states.

B. The four-qubit stabilizer states classification

The n -qubit Clifford group \mathcal{C}_n is the group of $n \times n$ unitary matrices that map the Pauli Group \mathcal{P}_n to itself under conjugation [32]. Two n -qubit states $|\psi\rangle$ and $|\psi'\rangle$ are Local Clifford (*LC*) equivalent if there exist operations C_1, C_2, \dots, C_n within the Clifford group such that

$$|\psi'\rangle = C_1 \otimes C_2 \otimes \dots \otimes C_n |\psi\rangle \quad (5)$$

Any stabilizer state is LC equivalent to some graph state [33], hence, the full space of n -qubit stabilizer states can be reached by applying LC operations to the full set of n -qubit graph states.

We trained the hybrid VQC to recognize the LC orbit of each of the four-qubit graph states represented in FIG. 4. This was done by first generating all 64 graph states and then applying random uniformly picked LC operations to generate samples of stabilizer states. The `random_clifford` function provided by Qiskit (v0.37) was used to create these LC operations. As before, the dataset was kept balanced: 50% of the sample stabilizer states were picked from the orbit to be learned and the other 50% were picked uniformly from the rest of the 5 orbits. TABLE V shows the results of the training and test accuracies for this case.

class N°	Training Accuracy	Test Accuracy
1	96%	97%
2	98%	98%
3	90%	90%
4	95%	95%
5	97%	97%
6	92%	91%

TABLE V: Training and test accuracy results for identification of entanglement classes of four-qubit stabilizer states.

class N°	Training Accuracy	Test Accuracy
1	94%	93%
2	95%	94%
3	90%	89%
4	95%	95%
5	90%	89%
6	90%	90%

TABLE VI: Training and test accuracy results for identification of LU orbits of four-qubit graph states.

It should be noted that until now the samples have been restricted to states within the LU equivalence classes of four-qubit graph states, and therefore the VQC is largely ignorant of states that do not fall into any of the six classes. In light of that, we also trained our classifier to recognize the LU orbits of four-qubit graph states from the entire four-qubit Hilbert space. For this purpose, 50% of the samples were taken from the LU equivalence class to be identified and the other 50% were random four-qubit states generated by choosing random complex values for all 16 elements of the amplitude vector. The training and test accuracies for this type of classification are shown in TABLE VII.

class N°	Training Accuracy	Test Accuracy
1	95%	94%
2	93%	91%
3	100%	99%
4	89%	88%
5	98%	97%
6	100%	99%

TABLE VII: Training and test accuracy results for identification of LU orbits of four-qubit graph states against the full four-qubit Hilbert space.

C. Identifying the *LU*-orbits of four-qubit graph states

We further trained the hybrid VQC to identify the LU orbits of four-qubit graph states. Since, LC group is a finite subset of the LU group, learning the LU orbits of quantum states is a much bigger task. Furthermore, the set of all states that can be reached by applying LU operations to graph states is continuous, and therefore this LU orbit contains an uncountable number of states. This identification of LU orbits is thus a big step up from the identification of LC orbits.

Similar to the LC case, first, all graph states were generated, followed by the application of randomly generated LU operators to create sample states from their LU orbit. The `unitary_group` statistical function from SciPy was used to generate Haar distributed random LU operators for this purpose. Once again, half of the samples were taken from the orbit to be identified and the rest from the other five orbits. The training and test accuracies for this case are shown in TABLE VI.

The results for this type of classification show better accuracy compared to those in TABLE VI for most of the classes. At first glance, this may appear counterintuitive, since Table VI presents a comparison between a single orbit and the other five four-qubit graph state LU-orbits, whereas Table VII compares one orbit with all remaining states. However, when a state is randomly selected from the four-qubit Hilbert space, it is typically a generic state whose entanglement pattern is most likely SLOCC-equivalent to the generic G_{abcd} four-qubit state, according to the classification of [11]. Therefore, in Table VII, the classifier is trained to distinguish between two types of entanglement, the chosen class and the generic one, whereas in Table VI, the dataset encompasses a wider variety of entanglement types. Consequently, the classifier performs significantly better when discriminating between two distinct types of entanglement than when

attempting to identify a specific type within a diverse set of entanglement structures.

V. CONCLUSION

In this paper we have presented a hybrid variational quantum circuit approach to entanglement classification. Our work shows that a hybrid VQC with post-processing through a classical NN does an excellent job of learning highly non-linear entanglement orbits. We demonstrated this for the case of four-qubit graph states by first showing that a hybrid VQC is able to correctly classify all possible four-qubit graph states into their six distinct equivalence classes with 98% accuracy or above. Following that, we show that this classifier is capable of recognizing and classifying all states in the LC orbit of these four-qubit graph states (the full finite set of stabilizer states) with 90% accuracy or higher. Finally, the classifier also shows excellent performance for the even more complicated task of learning the LU orbits of these four-qubit graph states. We show that the hybrid VQC can learn to identify states from each of the six equivalence classes with accuracy $\geq 88\%$.

These results highlight the robustness of our approach, especially when scaled up to more complicated classification schemes. Furthermore, the advantages of this approach, which include the lack of a need for full information of the quantum system, polynomial scaling of resources with the number of subsystems, and ready ex-

ecution on currently available NISQ era hardware, make it an extremely effective and practically useful method of entanglement classification when combined with the high accuracy of our results. A review of prior work on the use of variational quantum classification methods for entanglement classification also highlights the uniqueness of our approach since training a hybrid VQC to learn non-linear orbits for classification, to our knowledge, has not been performed yet.

Several avenues remain open for future research in this area. First, the scalability of our approach to larger systems needs to be addressed. Furthermore, while our research focused on graph states, this approach could be extended to the more tractable and commonly used SLOCC classification of all pure states. Finally, the performance of this classifier on actual quantum hardware and the corresponding impacts of noise and decoherence on its performance need to be explored. Investigating these possibilities could provide new insights into the practical classification of entangled states and its myriad applications in quantum information.

Acknowledgement

This work was supported by the Graduate school EIPHI (contract ANR-17-EURE- 0002) and the QuanTEEM Erasmus Master program. All codes are available at <https://github.com/Hamna-Aslam3/HybridVQC-stabilizer-state-classification>.

-
- [1] Ekert, A. K. (1991). Quantum cryptography based on Bell's theorem. *Physical Review Letters*, 67, 661–663.
- [2] Bennett, C. H., Brassard, G., Crépeau, C., Jozsa, R., Peres, A., & Wootters, W. K. (1993). Teleporting an unknown quantum state via dual classical and Einstein–Podolsky–Rosen channels. *Physical Review Letters*, 70(13), 1895–1899.
- [3] Calderbank, A. R., & Shor, P. W. (1996). Good quantum error-correcting codes exist. *Physical Review A*, 54(2), 1098–1105.
- [4] Grover, L. K. (1997). Quantum mechanics helps in searching for a needle in a haystack. *Physical Review Letters*, 79(2), 325–328.
- [5] Shor, P. W. (1997). Polynomial-time algorithms for prime factorization and discrete logarithms on a quantum computer. *SIAM Journal on Computing*, 26(5), 1484–1509.
- [6] Eltschka, C., & Siewert, J. (2014). Quantifying entanglement resources. *Journal of Physics A: Mathematical and Theoretical*, 47(42), 424005.
- [7] Wang, K., Song, Z., Zhao, X., Wang, Z., & Wang, X. (2022). Detecting and quantifying entanglement on near-term quantum devices. *npj Quantum Information*, 8(1), 52.
- [8] Rangamani, M., & Rota, M. (2015). Entanglement structures in qubit systems. *Journal of Physics A: Mathematical and Theoretical*, 48(38), 385301.
- [9] Acín, A., Andrianov, A., Costa, L., Jané, E., Latorre, J. I., & Tarrach, R. (2000). Generalized Schmidt decomposition and classification of three-quantum-bit states. *Physical Review Letters*, 85(7), 1560.
- [10] Dür, W., Vidal, G., & Cirac, J. I. (2000). Three qubits can be entangled in two inequivalent ways. *Physical Review A*, 62(6), 062314.
- [11] Verstraete, F., Dehaene, J., De Moor, B., & Verschelde, H. (2002). Four qubits can be entangled in nine different ways. *Physical Review A*, 65(5), 052112.
- [12] Jaffali, H., & Oeding, L. (2020). Learning algebraic models of quantum entanglement. *Quantum Information Processing*, 19(9), 279.
- [13] Asif, N., Khalid, U., Khan, A., Duong, T. Q., & Shin, H. (2023). Entanglement detection with artificial neural networks. *Scientific Reports*, 13(1), 1562.
- [14] Paris, M. G. A., & Řeháček, J. (Eds.). (2004). *Quantum state estimation*. Berlin, Heidelberg: Springer. ISBN 978-

- 3-540-22329-0.
- [15] Bae, J., & Kwek, L.-C. (2015). Quantum state discrimination and its applications. *Journal of Physics A: Mathematical and Theoretical*, 48(8), 083001.
 - [16] Schatzki, L., Arrasmith, A., Coles, P. J., & Cerezo, M. (2021). Entangled datasets for quantum machine learning. arXiv preprint arXiv:2109.03400.
 - [17] Scala, F., Mangini, S., Macchiavello, C., Bajoni, D., & Gerace, D. (2022). Quantum variational learning for entanglement witnessing. In 2022 International Joint Conference on Neural Networks (IJCNN) (pp. 1–8). IEEE.
 - [18] Qiu, P.-H., Chen, X.-G., & Shi, Y.-W. (2019). Detecting entanglement with deep quantum neural networks. *IEEE Access*, 7, 94310–94320.
 - [19] Grant, E., Benedetti, M., Cao, S., Hallam, A., Lockhart, J., Stojevic, V., Green, A. G., & Severini, S. (2018). Hierarchical quantum classifiers. *npj Quantum Information*, 4(1), 65.
 - [20] Wang, S., Shen, Y., Liu, X., Zhang, H., & Wang, Y. (2024). Variational quantum entanglement classification discrimination. *Physica A: Statistical Mechanics and its Applications*, 637, 129530.
 - [21] Mitarai, K., Negoro, M., Kitagawa, M., & Fujii, K. (2018). Quantum circuit learning. *Physical Review A*, 98(3), 032309.
 - [22] Nielsen, M. A., & Chuang, I. L. (2010). Quantum computation and quantum information. Cambridge university press.
 - [23] Holweck, F., Luque, J. G., & Thibon, J. Y. (2014). Entanglement of four qubit systems: A geometric atlas with polynomial compass I (the finite world). *Journal of Mathematical Physics*, 55(1).
 - [24] Holweck, F., Luque, J. G., & Thibon, J. Y. (2017). Entanglement of four-qubit systems: a geometric atlas with polynomial compass II (the tame world). *Journal of Mathematical Physics*, 58(2).
 - [25] Luque, J. G., & Thibon, J. Y. (2005). Algebraic invariants of five qubits. *Journal of physics A: mathematical and general*, 39(2), 371.
 - [26] Turner, J., & Morton, J. (2017). A complete set of invariants for LU-equivalence of density operators. *Symmetry, Integrability and Geometry: Methods and Applications*, 13, 028.
 - [27] Schuld, M., Bocharov, A., Svore, K. M., & Wiebe, N. (2020). Circuit-centric quantum classifiers. *Physical Review A*, 101(3), 032308.
 - [28] Rath, M., & Date, H. (2024). Quantum data encoding: a comparative analysis of classical-to-quantum mapping techniques and their impact on machine learning accuracy. *EPJ Quantum Technology*, 11, 72.
 - [29] Hein, M., Dür, W., Eisert, J., Raussendorf, R., Nest, M., & Briegel, H. J. (2006). Entanglement in graph states and its applications. arXiv preprint quant-ph/0602096.
 - [30] Markham, D., & Sanders, B. C. (2008). Graph states for quantum secret sharing. *Physical Review A—Atomic, Molecular, and Optical Physics*, 78(4), 042309.
 - [31] Cabello, A., Danielsen, L. E., López-Tarrida, A. J., & Portillo, J. R. (2011). Optimal preparation of graph states. *Physical Review A—Atomic, Molecular, and Optical Physics*, 83(4), 042314.
 - [32] Zeng, B., Chung, H., Cross, A. W., & Chuang, I. L. (2007). Local unitary versus local Clifford equivalence of stabilizer and graph states. *Physical Review A*, 75(3), 032325.
 - [33] Van den Nest, M., Dehaene, J., & De Moor, B. (2004). Graphical description of the action of local Clifford transformations on graph states. *Physical Review A*, 69(2), 022316.
 - [34] Claudet, N., & Perdrix, S. (2025). Deciding Local Unitary Equivalence of Graph States in Quasi-Polynomial Time. arXiv preprint arXiv:2502.06566.
 - [35] False for $n = 27$ qubits but true for $n \leq 19$ [34]